

# Chemistry–A European Journal

Supporting Information

## **Group 6 Hexacarbonyls as Ligands for the Silver Cation: Syntheses, Characterization, and Analysis of the Bonding Compared with the Isoelectronic Group 5 Hexacarbonylates**

Jan Bohnenberger,<sup>[a]</sup> Daniel Kratzert,<sup>[a]</sup> Sai Manoj N. V. T. Gorantla,<sup>[b]</sup> Sudip Pan,<sup>[b]</sup>  
Gernot Frenking,<sup>\*[b, c]</sup> and Ingo Krossing<sup>\*[a]</sup>

## Contents

Experimental Section .....	2
Synthesis of $[\text{Ag}\{\text{W}(\text{CO})_6\}_2][\text{F}-\{\text{Al}(\text{OR}^{\text{F}})_3\}_2]$ .....	4
Synthesis of $[\text{Ag}\{\text{Mo}(\text{CO})_6\}_2][\text{F}-\{\text{Al}(\text{OR}^{\text{F}})_3\}_2]$ .....	5
Summary of the crystallographic details of the compounds. ....	7
EDA-NOCV results .....	8
References to the S.I. ....	20

## Experimental Section

**General Conditions.** All manipulations on substrates and products were undertaken in a MBraun glovebox filled with Ar or N<sub>2</sub> (O<sub>2</sub>, H<sub>2</sub>O < 1 ppm). All experiments were carried out in special double-Schlenk tubes (S-S-Figure 1) separated by a G3 or G4 frit with grease-free PTFE or glass valves in an inert atmosphere using vacuum and standard Schlenk techniques. Solvents were dried by standard methods using CaH<sub>2</sub> or P<sub>4</sub>O<sub>10</sub> and distilled prior to use.

**NMR Spectroscopy.** NMR samples were prepared in 5 mm thick walled NMR tubes with J. Young valves. The <sup>1</sup>H, <sup>13</sup>C{<sup>1</sup>H}, <sup>19</sup>F and <sup>27</sup>Al spectra were recorded either on a Bruker Avance II+ 400 MHz, on a Bruker Avance III HD 300 MHz or on a Bruker Avance 200 MHz spectrometer either in 1,2-F<sub>2</sub>C<sub>6</sub>H<sub>4</sub> (*ortho*-difluorobenzene, *o*DFB) or CD<sub>2</sub>Cl<sub>2</sub> (0.4-0.6 mL) at r.t. Measurements conducted in 1,2-F<sub>2</sub>C<sub>6</sub>H<sub>4</sub> were calibrated by using the <sup>19</sup>F signal of the solvent 1,2-F<sub>2</sub>C<sub>6</sub>H<sub>4</sub> ( $\delta = -139.0$  ppm<sup>[1]</sup>, rel. to CCl<sub>3</sub>F). The field corrections of other nuclei were adjusted accordingly. Measurements conducted in 1,2,3,4-F<sub>4</sub>C<sub>6</sub>H<sub>2</sub> were calibrated to the residual solvent signal for <sup>1</sup>H ( $\delta = 7.04$  ppm<sup>[2]</sup>, rel. to TMS). The field corrections of other nuclei were adjusted accordingly. The Bruker Topspin software package (version 3.2) was used for measuring and processing of the spectra. Typically, very tiny impurities were detected in the <sup>19</sup>F NMR at -74.8 (HOC(CF<sub>3</sub>)<sub>3</sub>) and -75.5 ppm. All graphical representations were performed using Topspin (version 3.5pl7).

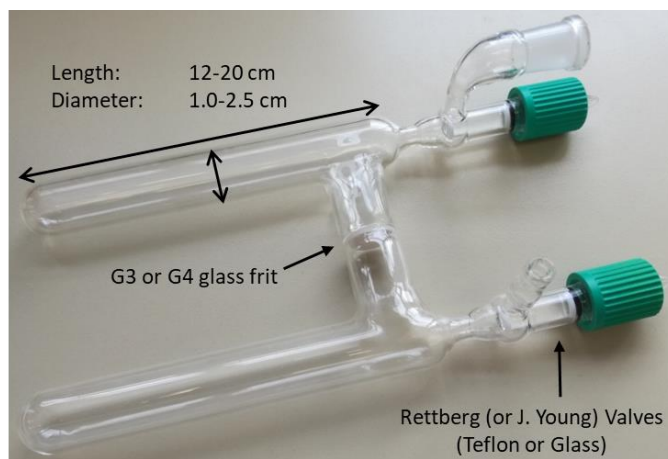
**Vibrational Spectroscopy.** FTIR measurements were performed on a FTIR Bruker ALPHA with a QuickSnap Platinum ATR sampling module inside the glovebox. The data were processed with the Bruker OPUS 7.5 software package. Unless otherwise stated, the spectra were recorded in the range of 4000-550 cm<sup>-1</sup> with a resolution of 2 cm<sup>-1</sup> at r.t. and a base line correction with 3 iterations was applied. FT Raman spectra were recorded on a Bruker VERTEX 70 spectrometer equipped with a RAM II module (1064 nm exciting line of a NdYAG laser) by using a highly sensitive liquid N<sub>2</sub> cooled Ge detector. The samples were measured in flame sealed soda-lime glass Pasteur pipettes in the range of 4000-50 cm<sup>-1</sup> with a resolution of 4 cm<sup>-1</sup> at r.t. The data were processed with the Bruker OPUS 7.5 software package. Unless otherwise noted, the Raman spectra were cut off below 75 cm<sup>-1</sup> and a baseline correction with 5 iterations was applied. All IR and Raman spectra were normalized to 1 and intensities are given as follows: vvw = very very weak (< 0.1), vw = very weak (< 0.2), w = weak (< 0.3), mw = medium weak (< 0.4), m = medium (< 0.5), ms = medium strong (< 0.6), s = strong (< 0.7), vs = very strong (< 0.8), vvs = very very strong ( $\geq 0.9$ ). Extremely weak bands (< 0.025) are not reported. Graphical representations have been done with OPUS 7.5.

**Single-Crystal X-ray Diffraction.** Single crystals were selected at r.t. under perfluoropolyalkylether oil (AB128330, ABCR GmbH & Co. KG) on 0.1, 0.2 or 0.3 mm micromounts (M1-L19-100/200/300).

Structural data were collected from shock-cooled crystals on either a Bruker SMART APEX II Quazar CCD area detector diffractometer using a D8 goniometer with an Incoatec Mo-Microfocus Source  $\mu\text{S}$  with mirror-monochromated Mo- $K_{\alpha}$  radiation ( $\lambda = 0.71073 \text{ \AA}$ ) at 100(2) with an Oxford Cryosystem 800 low temperature device or with a Bruker D8 VENTURE with PHOTONIII Detector, Fixed-Chi D8 Goniometer, INCOATEC Mo/Cu Microsource and Oxford Cryostream 800 low temperature device. The data were processed with APEX v2013.6-2, integrated with SAINT<sup>[3]</sup> (V8.37A) and an empirical absorption correction using SADABS 2014/5<sup>[4]</sup> or SADABS 2016/2<sup>[4]</sup> was applied. The structures were solved by direct methods using SHELXT<sup>[5,6]</sup>. Unless otherwise stated, all non-hydrogen atoms were refined anisotropically by full matrix least squares methods against weighted  $F^2$  values based on all independent reflections by using SHELXL-2014/7<sup>[6,7]</sup> with ShelXle as GUI software<sup>[8]</sup>. Disordered fragments were modelled with the help of the DSR software<sup>[9]</sup>. The graphical presentation of crystal structures was prepared either with Mercury (version 3.9)<sup>[10]</sup> or with OLEX2 (version 1.2).<sup>[11]</sup>

**Powder Diffraction.** The powder diffractograms were recorded with the sample in a 0.5 mm thick capillary (Hilgenberg GmbH, wall thickness 0.01 mm) sealed with perfluoropolyalkylether oil (AB128330, ABCR GmbH & Co. KG), at RT and about 100(10) K in the  $2-\Theta$  range  $2-44^\circ$  with a STOE STADI P powder diffractometer with Mo- $K_{\alpha 1}$  radiation ( $\lambda = 0.709300 \text{ \AA}$ ) equipped with a Ge-(111) monochromator and a silicon microstripe detector (Mythen 1K). Data acquiring, processing and the calculation of powder diffractograms from single-crystal data were performed using STOE WinXPOW<sup>®</sup> package.

**Computational Details.** Quantum chemical calculations<sup>[12]</sup> were performed with the Turbomole<sup>[12]</sup> program package (version 7.0). All investigated molecular structures were optimized at the density functional theory (DFT) and were run in redundant internal coordinates using the BP86<sup>[13]</sup> functional with the resolution-of-identity (RI) approximation<sup>[14]</sup> together with the basis set def2-TZVPP<sup>[15]</sup> and with dispersion correction (DFT-D3BJ)<sup>[16]</sup>. A fine integration grid (m4) and the default SCF convergence criteria ( $10^{-6}$  a.u.) were used. All optimized structures were checked for minima (no imaginary frequencies) with the implemented module AOforce<sup>[17]</sup> and for proper spin occupancies using the implemented module Eiger. Entropic contributions to enthalpy and Gibbs free energy with inclusion of zero-point energies (ZPE) were calculated at the BP86-D3BJ/def2-TZVPP level for standard conditions with the FreeH module.



**S-Figure 1.** Double-Schlenk tube that was typically used for most reactions and crystallizations. Note that different varieties (sizes, Rettberg or J. Young valves) were used.

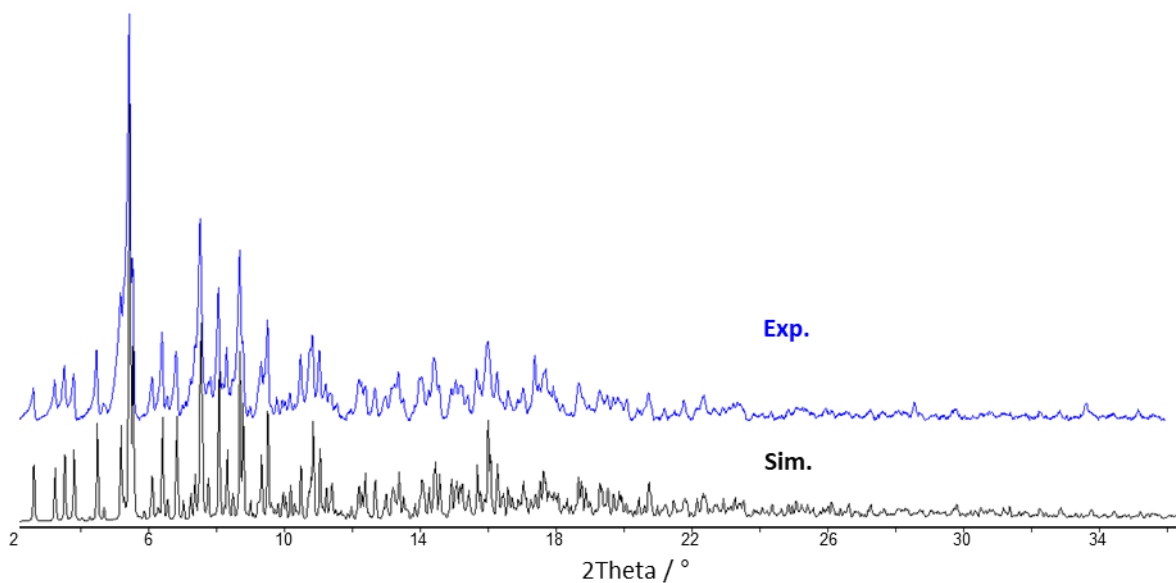
### Synthesis of $[\text{Ag}\{\text{W}(\text{CO})_6\}_2][\text{F}-\{\text{Al}(\text{OR}^{\text{F}})_3\}_2]$

Inside the glove box, a double-Schlenk tube was equipped with  $\text{W}(\text{CO})_6$  (75 mg, 0.213 mmol, 2 eq) and  $\text{Ag}[\text{F}-\{\text{Al}(\text{OR}^{\text{F}})_3\}_2]$  (170 mg, 0.107 mmol) and  $\text{C}_6\text{F}_6$  (10 mL) was added. A slight yellow suspension yielded, which was stirred overnight. The next day, colorless precipitate was visible and the volatiles were removed. Addition of TFB (3 mL) led to a dark solution, which turned clear after five minutes. The solution was filtered and crystallized by slow vapor diffusion of *n*-pentane, which led to pale-yellow crystals of  $[\text{Ag}\{\text{W}(\text{CO})_6\}_2][\text{F}-\{\text{Al}(\text{OR}^{\text{F}})_3\}_2]$ . Yield: 180 mg, 86%.

The powder XRD at 100K showed no crystalline impurities.

**FTIR** (ZnSe, ATR):  $\tilde{\nu}/\text{cm}^{-1}$  (intensity) = 2129 (mw), 2074 (m), 1998 (s, br), 1354 (vw), 1301 (mw), 1277 (ms), 1267 (ms), 1243 (vvs), 1213 (vvs), 1174 (ms), 973 (vvs), 863 (vw), 760 (vww), 727 (vvs), 639 (w), 561 (m).

**FT Raman** (500 scans, 500 mW,  $4\text{ cm}^{-1}$ ):  $\tilde{\nu}/\text{cm}^{-1}$  (intensity) = 2173 (vww), 2142 (mw), 2044 (vww), 2076 (vvs), 2020 (vw), 1983 (vww), 1304 (vww), 1280 (vww), 1141 (vww), 981 (vww), 814 (vww), 753 (vw), 572 (vww), 539 (vww), 500 (vww), 482 (vww), 413 (mw), 363 (vww), 325 (vww), 292 (vww), 234 (vww), 102 (ms).



**S-Figure 2.** 100K powder XRD of  $[\text{Ag}\{\text{W}(\text{CO})_6\}_2][\text{F}-\{\text{Al}(\text{OR}^{\text{F}})_3\}_2]$  (blue) in comparison with the simulated diffractogram (black).

### Synthesis of $[\text{Ag}\{\text{Mo}(\text{CO})_6\}_2][\text{F}-\{\text{Al}(\text{OR}^{\text{F}})_3\}_2]$

Inside the glove box, a double-Schlenk tube was equipped with  $\text{Mo}(\text{CO})_6$  (30 mg, 0.114 mmol, 2 eq) and  $\text{Ag}[\text{F}-\{\text{Al}(\text{OR}^{\text{F}})_3\}_2]$  (90 mg, 0.057 mmol) and  $\text{C}_6\text{F}_6$  (3 mL) was added. A slight yellow suspension yielded, which was stirred for two hours. Then, the volatiles were removed and the addition of TFB (3 mL) led to a slightly yellow solution. The solution was filtered and crystallized by slow vapor diffusion of *n*-pentane, which led to colorless crystals of  $[\text{Ag}\{\text{Mo}(\text{CO})_6\}_2][\text{F}-\{\text{Al}(\text{OR}^{\text{F}})_3\}_2]$ . The isolated (dry) crystals decompose rapidly in Ar atmosphere, thus no yield determination was possible.

**FT Raman** (100 scans, 50 mW,  $4 \text{ cm}^{-1}$ ):  $\tilde{\nu}/\text{cm}^{-1}$  (intensity) = 2142 (m), 2114 (w), 2083 (vvs), 2024 (mw), 2005 (s), 1307 (vw), 814 (vw), 753 (vw), 464 (vww), 388 (w), 321 (vw), 103 (ms).

**S-Table 1.** Full assignment of all IR and Raman vibrations for  $[\text{Ag}\{\text{Mo}(\text{CO})_6\}_2][\text{F}-\{\text{Al}(\text{OR}^{\text{F}})_3\}_2]$  and  $[\text{Ag}\{\text{W}(\text{CO})_6\}_2][\text{F}-\{\text{Al}(\text{OR}^{\text{F}})_3\}_2]$ .

$[\text{Ag}\{\text{Mo}(\text{CO})_6\}_2]^+$ calcd. <sup>a)</sup>		$[\text{Ag}\{\text{Mo}(\text{CO})_6\}_2]$ $[\text{F}-\{\text{Al}(\text{OR}^{\text{F}})_3\}_2]$	$[\text{Ag}\{\text{W}(\text{CO})_6\}_2]$ $[\text{F}-\{\text{Al}(\text{OR}^{\text{F}})_3\}_2]$	$[\text{Ag}\{\text{W}(\text{CO})_6\}_2]^+$ calcd. <sup>a)</sup>		$[\text{F}-\{\text{Al}(\text{OR}^{\text{F}})_3\}_2]^-$ [18]	Assignment <sup>(18) b)</sup>	
IR	Raman	Raman	Raman	IR	IR	Raman	IR	
	7 (vvw)					6 (vvw)		$\delta(\text{W}/\text{Mo}-\text{C})$ A
	25 (vww)					24 (vww)		$\delta(\text{W}/\text{Mo}-\text{C})$ A
	59 (vw)					57 (vw)		$\delta(\text{W}/\text{Mo}-\text{C})$ A
	79 (vvs)	103 (ms)	102 (ms)			80 (vvs)		$\delta(\text{W}/\text{Mo}-\text{C})$ A *
	106 (vw)					96 (w)		$\nu(\text{W}/\text{Mo}-\text{Ag})$ A
	129 (vww)					125 (vww)		$\delta(\text{W}/\text{Mo}-\text{C})$ A/B
			234 (vww)					- [Anion]
			292 (vww)					- [Anion]
		321 (vw)	325 (vww)					- [Anion]
377 (vww)	368 (vw)		363 (vww)		369 (vww)	365 (vww)		$\nu(\text{W}/\text{Mo}-\text{C})$ A + B *
393 (vww)								$\nu(\text{Mo}-\text{C})$ A + B
405 (vww)	408 (ms)	388 (w)			402 (vww)	403 (vw)		$\nu(\text{W}/\text{Mo}-\text{C})$ A + B *
			413 (mw)		419 (vww)	421 (m)		$\nu(\text{W}-\text{C})$ A + B *
			482 (vww)			483 (vww)		$\delta(\text{W}-\text{C})$ A *
498 (vww)	502 (m)	464 (vww)	500 (vww)		502 (vww)	506 (ms)		$\delta(\text{W}/\text{Mo}-\text{C})$ A + B *
					562 (vw)	567 (vww)		$\delta(\text{W}-\text{C})$ A + B
			539 (vww)					C-C, C-O
			572 (vww)	561 (m)			572 (m)	- [Anion]
584 (w)								$\delta(\text{Mo}-\text{C})$ A
	593 (vww)							Al-F-Al
				639 (w)			639 (m)	C-C, C-O
				727 (vvs)			728 (s)	- [Anion]
		753 (vw)	753 (vw)					C-C, C-O
				760 (vww)				- [Anion]
		814 (vw)	814 (vww)					Al-O, Al-F-Al
				853 (vw)			865 (w)	C-C, C-F
				973 (vvs)			975 (s)	- [Anion]
			981 (vww)					C-C, C-O
			1141 (vww)					C-C, C-F
				1174 (ms)			1183 (m)	C-C, C-F
				1213 (vvs)			1218 (s)	C-C, C-F
				1243 (vvs)			1249 (s)	C-C, C-F
				1267 (ms)			1268 (m)	C-C, C-F
			1280 (vww)	1277 (ms)				C-C, C-F
		1307 (vww)	1304 (vww)	1301 (mw)			1301 (m)	C-C, C-F
				1354 (vw)			1355 (m)	C-C, C-F
1966 (w)			1983 (vww)	1998 (s, br)	1961 (w)	1961 (vww)		$\nu(\text{C}-\text{O})$ A
1977 (s)	1977 (vww)	2005 (s)	2020 (vw)		1973 (s)	1973 (vw)		$\nu(\text{C}-\text{O})$ A
2033 (vvs)	2032 (vww)	2024 (mw)	2044 (vww)		2027 (vvs)	2026 (vww)		$\nu(\text{C}-\text{O})$ A + B
2058 (mw)	2058 (mw)			2074 (m)	2052 (mw)	2052 (mw)		$\nu(\text{C}-\text{O})$ A + B
2070 (mw)	2070 (w)	2083 (vww)	2076 (vvs)		2065 (mw)	2065 (w)		$\nu(\text{C}-\text{O})$ A
2113 (ms)		2114 (w)		2129 (mw)	2111 (ms)			$\nu(\text{C}-\text{O})$ B
	2128 (vw)	2142 (m)	2142 (mw)			2126 (vw)		$\nu(\text{C}-\text{O})$ A
			2173 (vww) <sup>c)</sup>					<sup>c)</sup>

<sup>a)</sup> BP86-D3BJ/def2-TZVPP,  $C_2$  symmetry, **no scale factor was applied**. w: weak, m: medium, s: strong, v: very, sh: shoulder, br: broad.

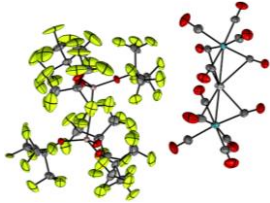
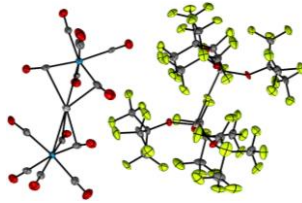
<sup>b)</sup> The assignments of the respective anion bands and their intensities are based on  $[\text{CBr}_3][\text{F}-\{\text{Al}(\text{OR}^{\text{F}})_3\}_2]$  (IR only) in ref.<sup>[18]</sup>.

<sup>c)</sup> The  $A_{1g}$  mode of the  $[\text{M}(\text{CO})_6]^+$  cations vibrates also at  $2173 \text{ cm}^{-1}$ , although this might be coincidental. A possible combination band  $975 \text{ cm}^{-1} + 1198 \text{ cm}^{-1}$  of the anion might also serve as an explanation.

\* The assignment is ambiguous.

## Summary of the crystallographic details of the compounds.

**S-Table 2.** Summary of the crystallographic details of the compounds.

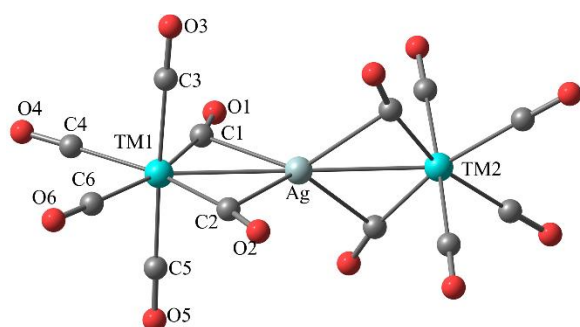
	[Ag{Mo(CO) <sub>6</sub> } <sub>2</sub> ][F-{Al(OR <sup>F</sup> ) <sub>3</sub> ] <sub>2</sub> ]	[Ag{W(CO) <sub>6</sub> } <sub>2</sub> ][F-{Al(OR <sup>F</sup> ) <sub>3</sub> ] <sub>2</sub> ]
		
CCDC number	2025555	2025554
Empirical formula	C <sub>36</sub> O <sub>18</sub> F <sub>55</sub> Al <sub>2</sub> Mo <sub>2</sub> Ag	C <sub>72</sub> O <sub>36</sub> F <sub>110</sub> Al <sub>4</sub> W <sub>4</sub> Ag <sub>2</sub>
Formula weight	2119.07	4589.78
Temperature/K	150.0	100.0
Crystal system	monoclinic	monoclinic
Space group	<i>P2<sub>1</sub>/n</i>	<i>P2<sub>1</sub>/n</i>
<i>a</i> /Å	13.137(9)	16.4875(10)
<i>b</i> /Å	14.915(10)	14.7946(9)
<i>c</i> /Å	32.38(2)	50.830(3)
$\alpha$ /°	90	90
$\beta$ /°	97.185(18)	91.608(2)
$\gamma$ /°	90	90
Volume/Å <sup>3</sup>	6295(7)	12393.8(13)
<i>Z</i>	4	4
$\rho_{\text{calc}}$ /cm <sup>3</sup>	2.236	2.4595
$\mu$ /mm <sup>-1</sup>	0.956	4.276
<i>F</i> (000)	4048.0	8601.3
Crystal size/mm <sup>3</sup>	0.2 × 0.1 × 0.05	0.15 × 0.1 × 0.1
Radiation	MoK $\alpha$ ( $\lambda$ = 0.71073)	Mo K $\alpha$ ( $\lambda$ = 0.71073)
2 $\theta$ range for data collection/°	2.536 to 56.666	1.6 to 52.9
Index ranges	-17 ≤ <i>h</i> ≤ 17, -19 ≤ <i>k</i> ≤ 19, -43 ≤ <i>l</i> ≤ 42	-20 ≤ <i>h</i> ≤ 20, -18 ≤ <i>k</i> ≤ 18, -63 ≤ <i>l</i> ≤ 63
Reflections collected	97067	283634
Independent reflections	15681 [R <sub>int</sub> = 0.0581, R <sub>sigma</sub> = 0.0419]	25526 [R <sub>int</sub> = 0.1368, R <sub>sigma</sub> = 0.0748]
Data/restraints/parameters	15681/16610/1591	25526/3225/2053
Goodness-of-fit on <i>F</i> <sup>2</sup>	1.064	1.171
Final <i>R</i> indexes [ <i>I</i> > 2 $\sigma$ ( <i>I</i> )]	R <sub>1</sub> = 0.0546, wR <sub>2</sub> = 0.1244	R <sub>1</sub> = 0.0752, wR <sub>2</sub> = 0.1255
Final <i>R</i> indexes [all data]	R <sub>1</sub> = 0.0907, wR <sub>2</sub> = 0.1435	R <sub>1</sub> = 0.1226, wR <sub>2</sub> = 0.1393
Largest diff. peak/hole / e Å <sup>-3</sup>	1.10/-0.81	2.12/-2.10



## EDA-NOCV results

**S-Table 3.** EDA-NOCV results of  $[\text{Ag}(\text{M}(\text{CO})_n)]$  complexes using three different sets of fragments with different charges and electronic states (S = singlet; D = doublet) and associated bond types at the BP86-D3(BJ)/TZ2P level. Energies are in kcal/mol. The most favourable fragmentation scheme and bond type is given by the smallest  $\Delta E_{\text{orb}}$  value written in red.

Molecule	Fragments	$\Delta E_{\text{int}}$	$\Delta E_{\text{Pauli}}$	$\Delta E_{\text{elstat}}$	$\Delta E_{\text{disp}}$	$\Delta E_{\text{orb}}$
$[\text{AgV}(\text{CO})_6]_2^-$	$[\text{Ag}]^+ (\text{S}) + [\text{V}(\text{CO})_6]_2^{2-} (\text{S})$	-257.2	148.7	-269.0	-15.4	<b>-121.5</b>
	$[\text{Ag}] (\text{D}) + [\text{V}(\text{CO})_6]_2^- (\text{D})$	-88.2	255.2	-186.2	-15.4	-141.7
	$[\text{Ag}]^- (\text{S}) + [\text{V}(\text{CO})_6]_2 (\text{S})$	-164.6	431.2	-326.4	-15.4	-254.0
$[\text{AgTa}(\text{CO})_6]_2^-$	$[\text{Ag}]^+ (\text{S}) + [\text{Ta}(\text{CO})_6]_2^{2-} (\text{S})$	-258.7	164.7	-285.7	-15.3	<b>-122.4</b>
	$[\text{Ag}] (\text{D}) + [\text{Ta}(\text{CO})_6]_2^- (\text{D})$	-89.6	269.4	-193.0	-15.3	-150.7
	$[\text{Ag}]^- (\text{S}) + [\text{Ta}(\text{CO})_6]_2 (\text{S})$	-176.8	462.3	-326.5	-15.3	-297.4
$[\text{AgNb}(\text{CO})_6]_2^-$	$[\text{Ag}]^+ (\text{S}) + [\text{Nb}(\text{CO})_6]_2^{2-} (\text{S})$	-256.2	149.7	-269.6	-14.8	<b>-122.2</b>
	$[\text{Ag}] (\text{D}) + [\text{Nb}(\text{CO})_6]_2^- (\text{D})$	-89.4	244.4	-184.9	-14.8	-134.1
	$[\text{Ag}]^- (\text{S}) + [\text{Nb}(\text{CO})_6]_2 (\text{S})$	-162.4	475.7	-356.6	-14.8	-266.6

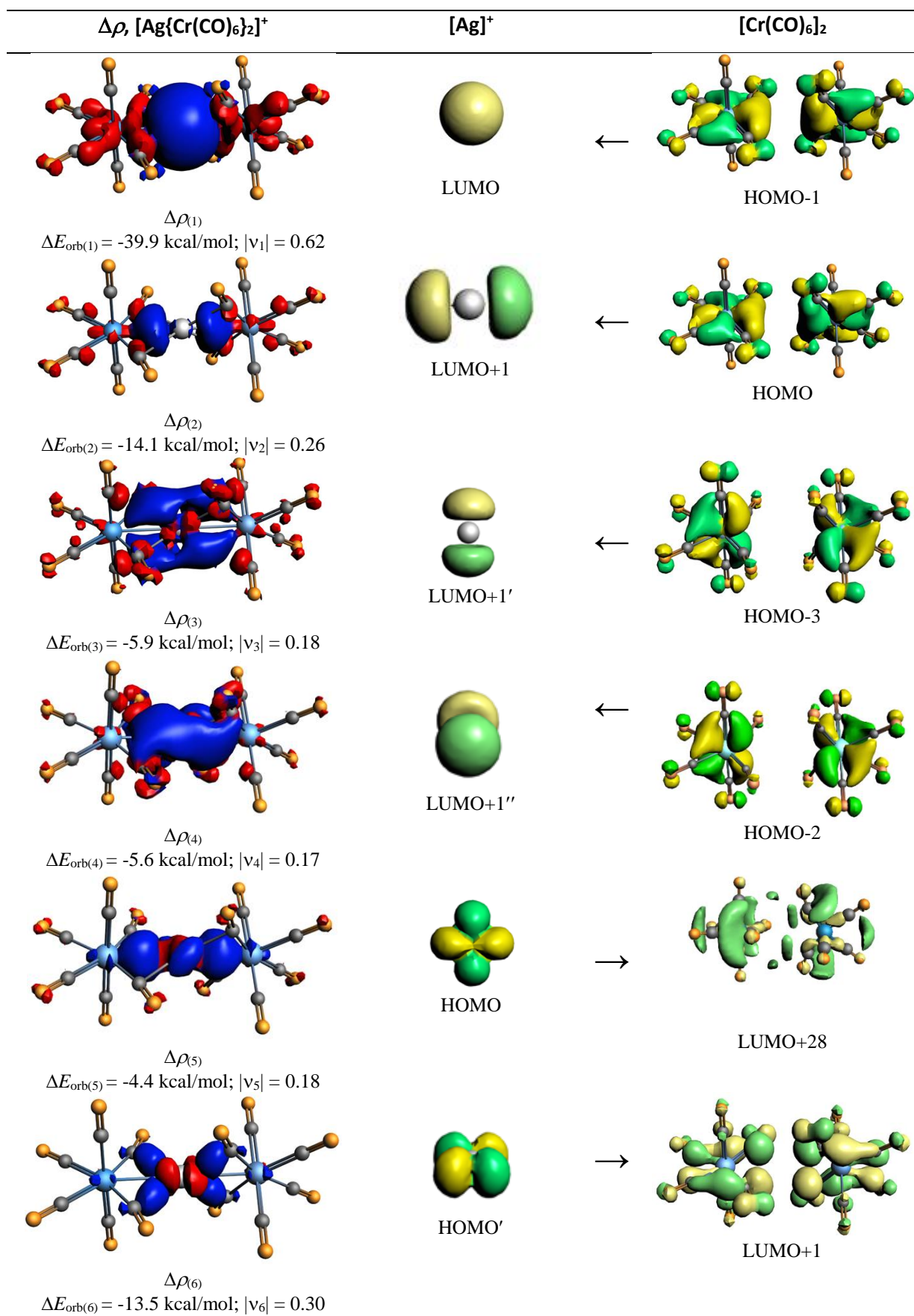


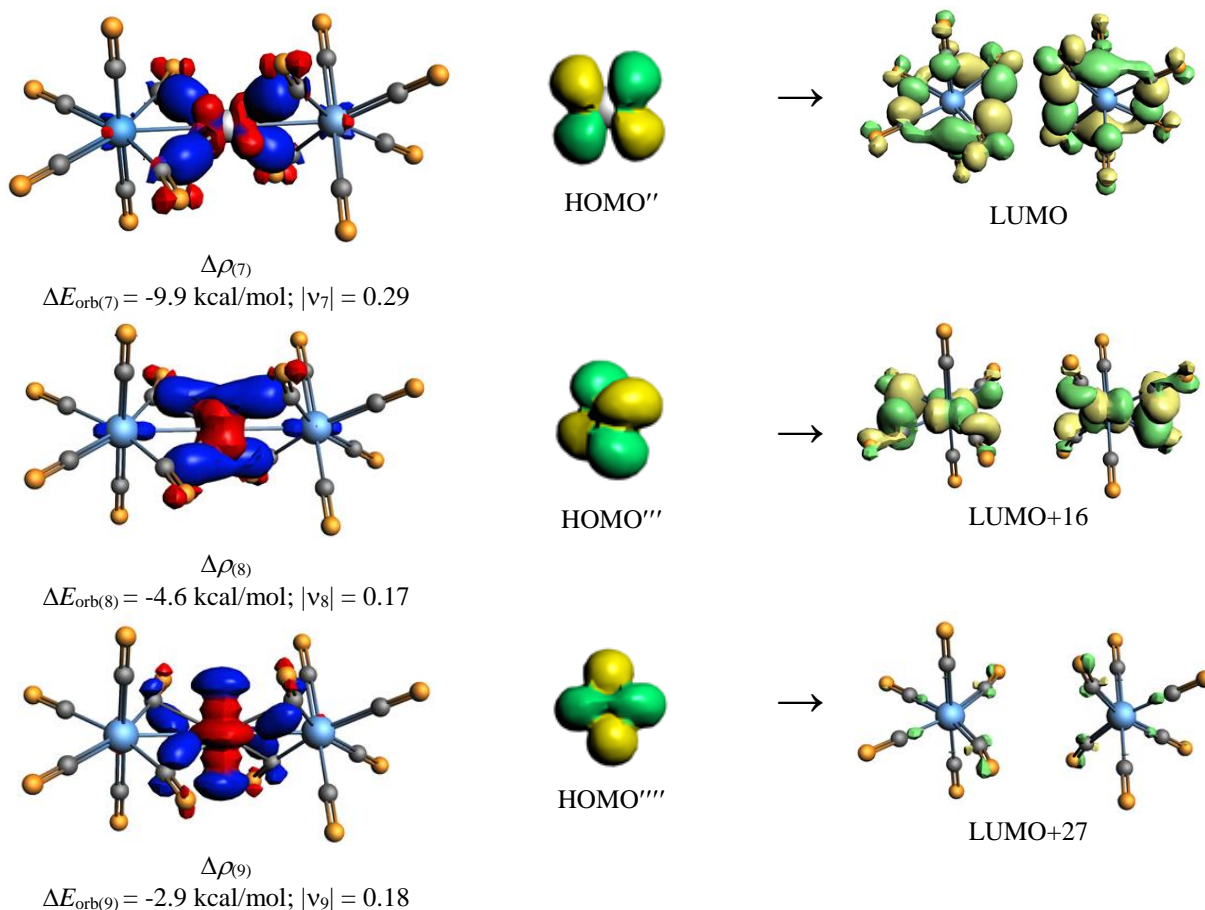
$[\text{Ag}\{\text{M}(\text{CO})_6\}_2]^+ (\text{M} = \text{Cr}, \text{Mo}, \text{W}) (\text{C}_2, ^1\text{A})$

	Cr	Mo	W
M1-Ag:	2.727	2.813(2.837) <sup>a</sup>	2.830(2.860) <sup>a</sup>
Ag-C1:	2.361	2.414(2.518)	2.429(2.466)
Ag-C2:	2.362	2.422(2.631)	2.439(2.685)
M1-C1:	1.931	2.071	2.082
M1-C2:	1.931	2.071	2.082
M1-C3:	1.920	2.067	2.077
M1-C4:	1.917	2.073	2.085
M1-C5:	1.920	2.067	2.077
M1-C6:	1.917	2.073	2.085
C1-O1:	1.157	1.156	1.157
C2-O2:	1.157	1.156	1.157
C3-O3:	1.146	1.146	1.147
C4-O4:	1.143	1.142	1.143
C5-O5:	1.146	1.146	1.147
C6-O6:	1.143	1.142	1.143
<M1-Ag-M2:	179.2	178.5	178.3

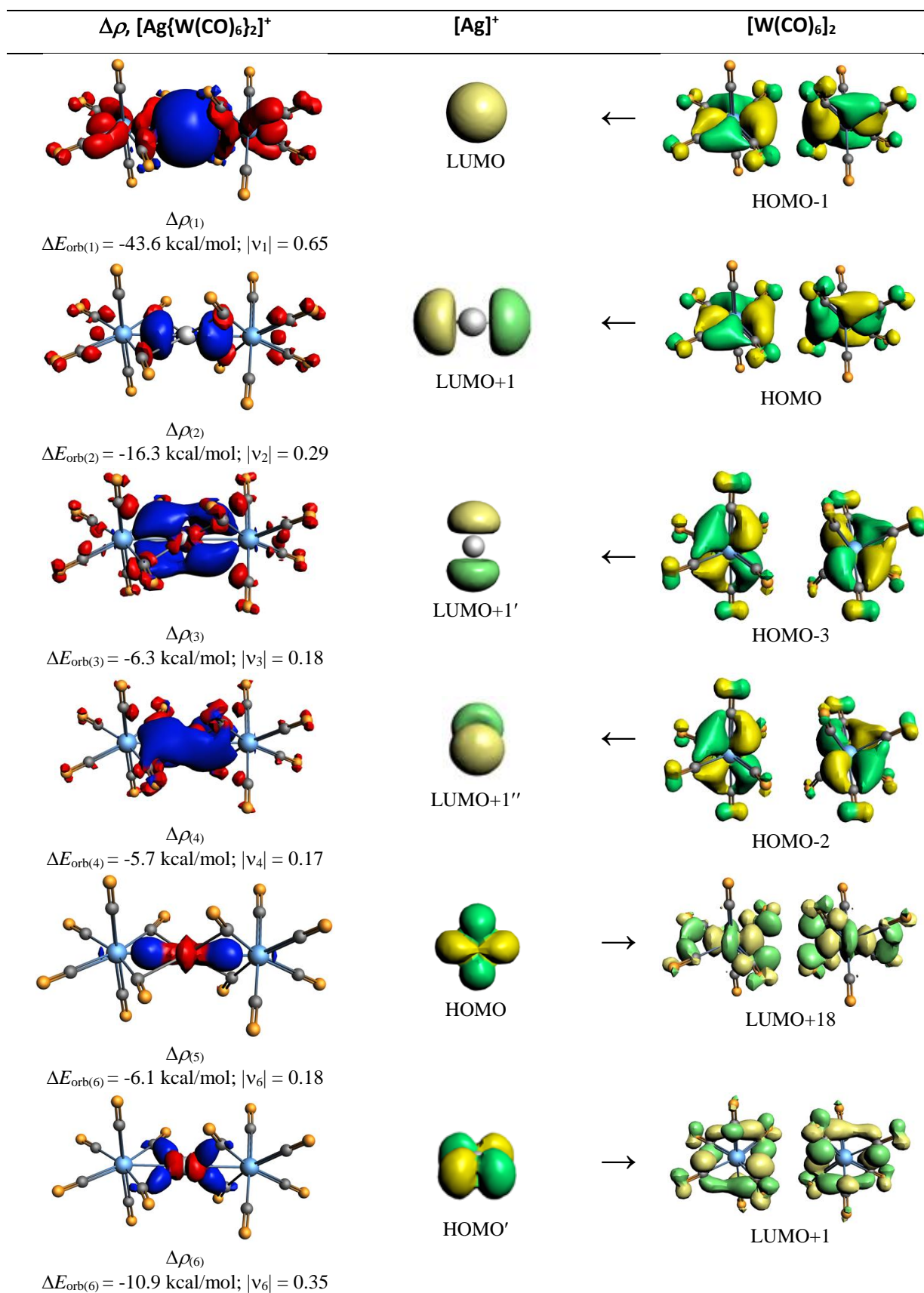
<sup>a</sup>Average value of slightly different data

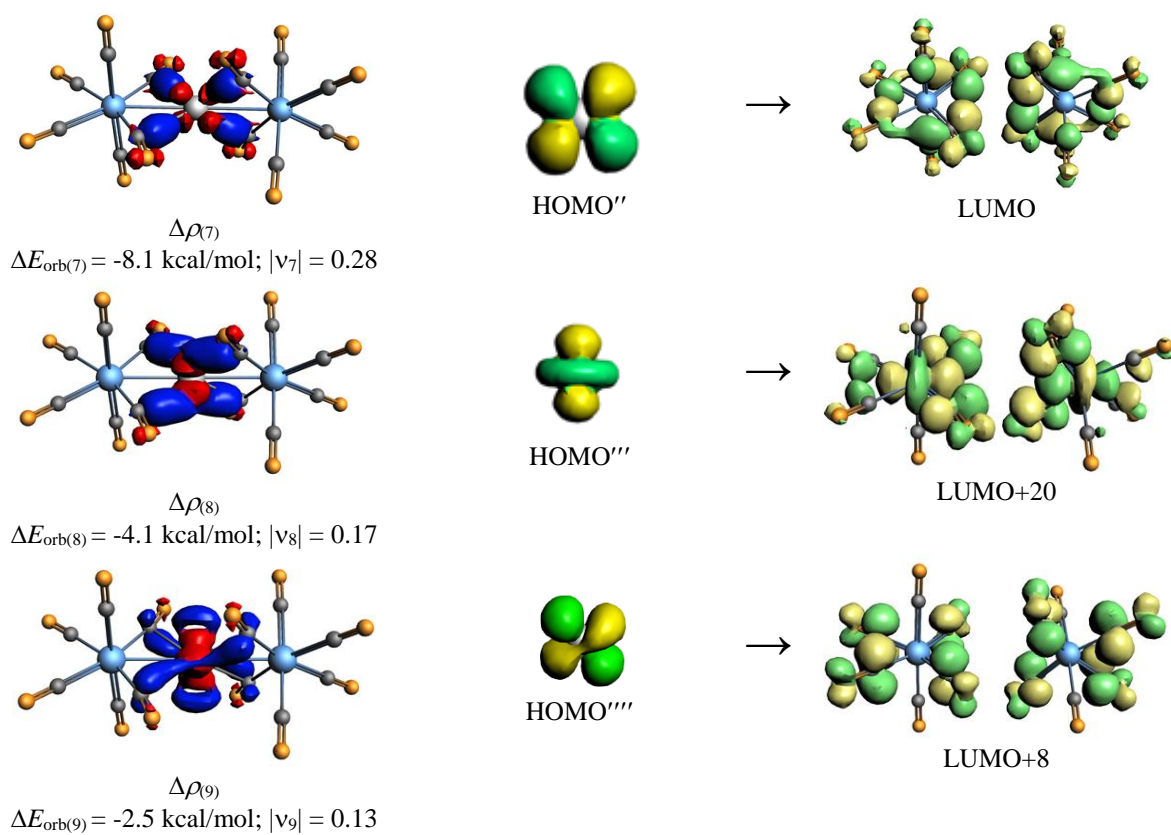
**S-Figure 3.** Calculated geometries of  $[\text{Ag}\{\text{M}(\text{CO})_6\}_2]^+$  (M = Cr, Mo, W) complexes at the BP86-D3(BJ)/def2-TZVPP level. Bond distances are in Å and angles are in degree. The experimental values are given in parentheses.



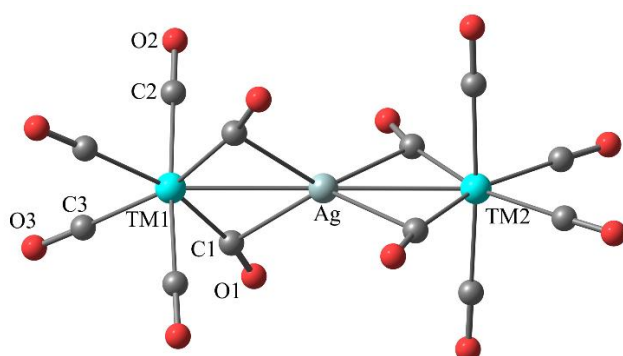


**S-Figure 4.** The shape of the deformation densities  $\Delta\rho_{(1)-(5)}$  that correspond to  $\Delta E_{\text{orb}(1)-(5)}$ , and the fragments orbitals of  $[\text{Ag}]^+$  and  $[\text{Cr}(\text{CO})_6]_2$  in the singlet state at the BP86-D3(BJ)/TZ2P level. Isosurface values are 0.001 au. The eigenvalues  $|v_n|$  give the size of the charge migration in e. The direction of the charge flow of the deformation densities is red→blue.



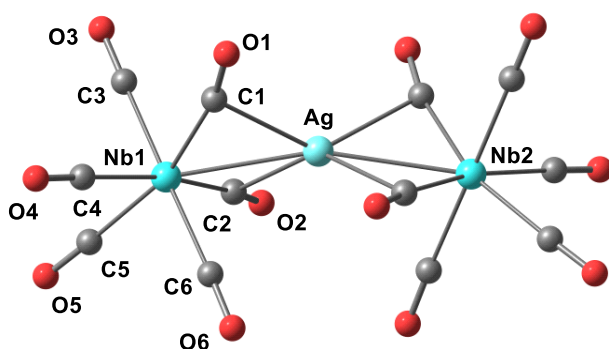


**S-Figure 5.** The shape of the deformation densities  $\Delta\rho_{(1)-(5)}$  that correspond to  $\Delta E_{\text{orb}(1)-(5)}$ , and the fragments orbitals of  $[\text{Ag}]^+$  and  $[\text{W}(\text{CO})_6]_2$  in the singlet state at the BP86-D3(BJ)/TZ2P level. Isosurface values are 0.001 au. The eigenvalues  $|v_n|$  give the size of the charge migration in e. The direction of the charge flow of the deformation densities is red→blue.



[Ag{M(CO)<sub>6</sub>}<sub>2</sub>]<sup>-</sup> (M = V, Ta) (*D*<sub>2h</sub>, <sup>1</sup>A)

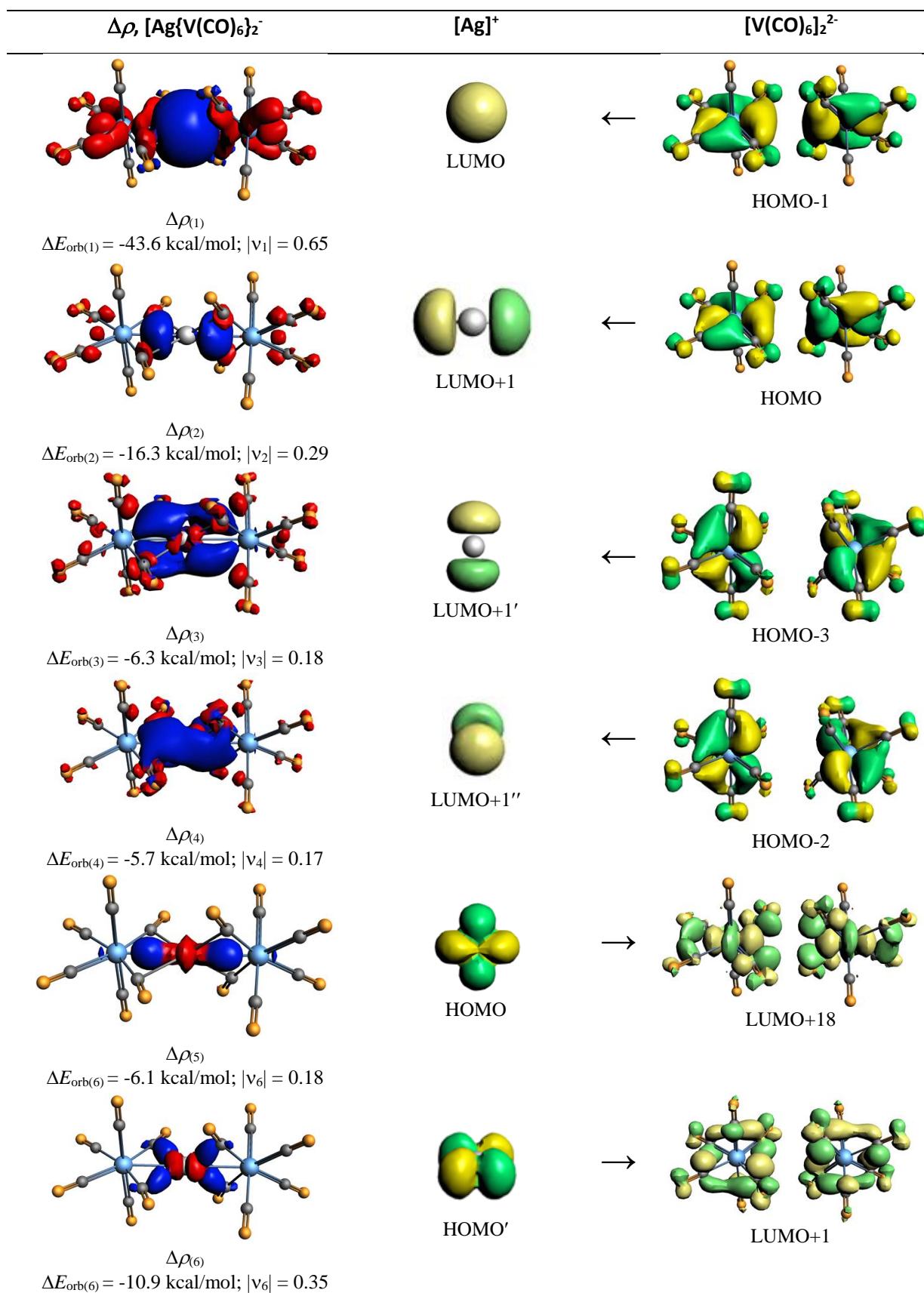
	V	Ta
M1-Ag:	2.732	2.848
Ag-C1:	2.469	2.387
M1-C1:	2.143	1.985
M1-C2:	2.130	1.965
M1-C3:	2.128	1.953
C1-O1:	1.168	1.169
C2-O2:	1.162	1.162
C3-O3:	1.161	1.161
<M1-Ag-M2:	180.0	180.0

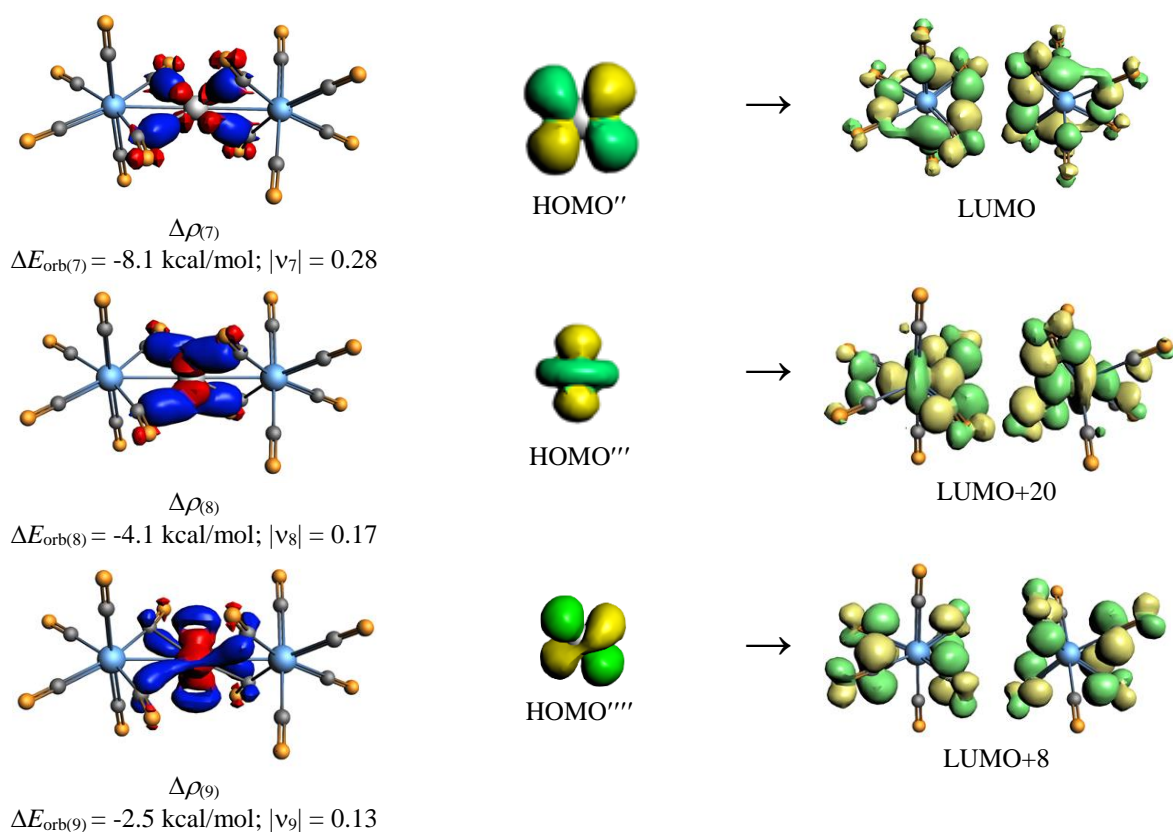


[Ag{Nb(CO)<sub>6</sub>}<sub>2</sub>]<sup>-</sup> (*C*<sub>2v</sub>, <sup>1</sup>A)

Nb-Ag:	2.818 (2.836, 2.847)
Ag-C1:	2.418 (2.544, 2.607)
Ag-C2:	2.571 (2.611, 2.669)
Nb1-C1:	2.140 (2.122, 2.138)
Nb1-C2:	2.143 (2.134, 2.111)
Nb1-C3:	2.137 (2.139, 2.136)
Nb1-C4:	2.123 (2.150, 2.150)
Nb1-C5:	2.122 (2.139, 2.133)
Nb1-C6:	2.125 (2.130, 2.138)
C1-O1:	1.169 (1.155, 1.152)
C2-O2:	1.164 (1.153, 1.157)
C3-O3:	1.161 (1.139, 1.137)
C4-O4:	1.160 (1.140, 1.139)
C5-O5:	1.162 (1.138, 1.139)
C6-O6:	1.160 (1.137, 1.146)
<Nb1-Ag-Nb2:	162.0 (174.0)

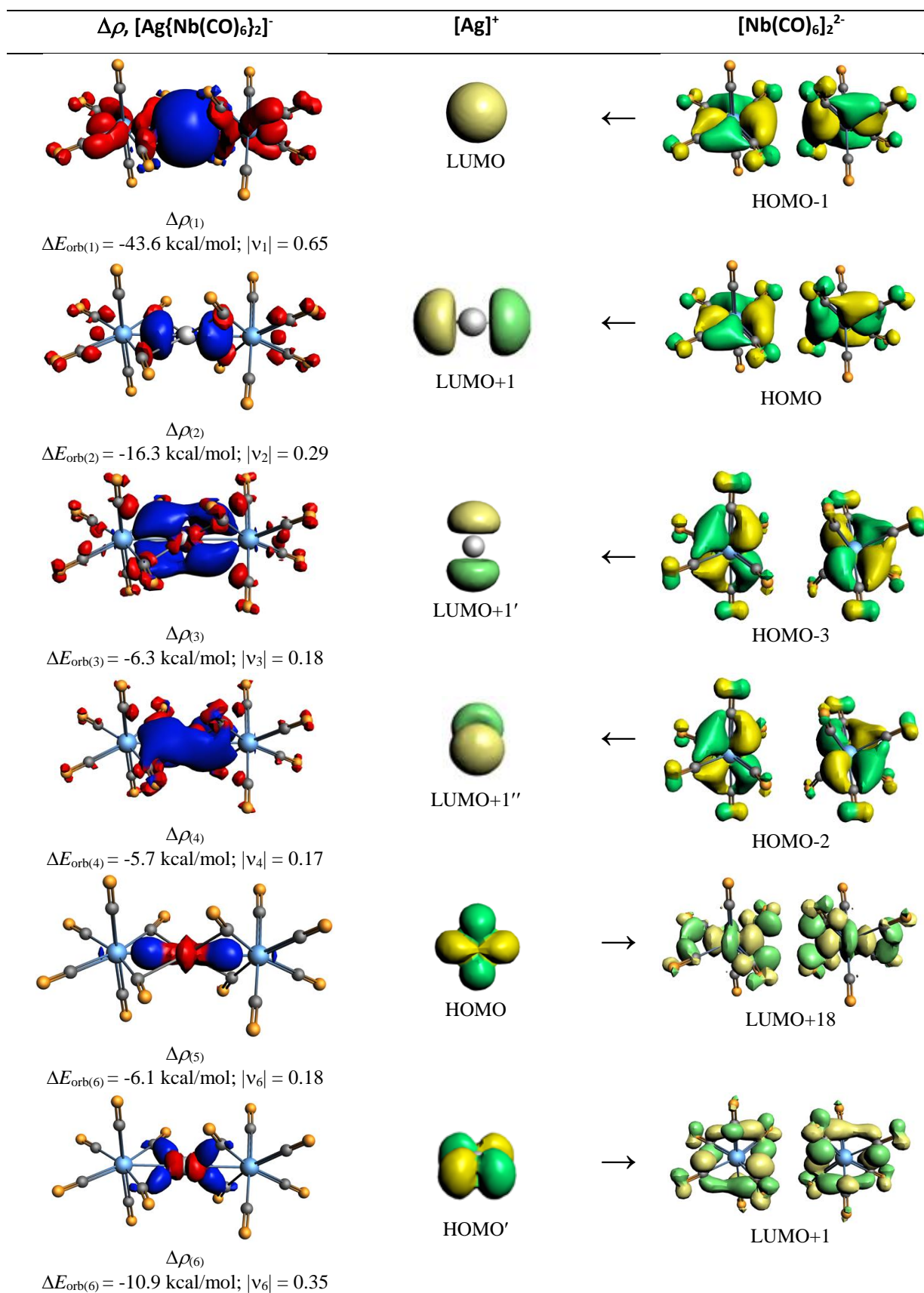
**S-Figure 6.** Calculated geometries of [Ag{M(CO)<sub>6</sub>}<sub>2</sub>]<sup>-</sup> (M = V, Nb, Ta) complexes at the BP86-D3(BJ)/def2-TZVPP level. Bond distances are in Å and angles are in degree. The experimental values are given in parentheses.

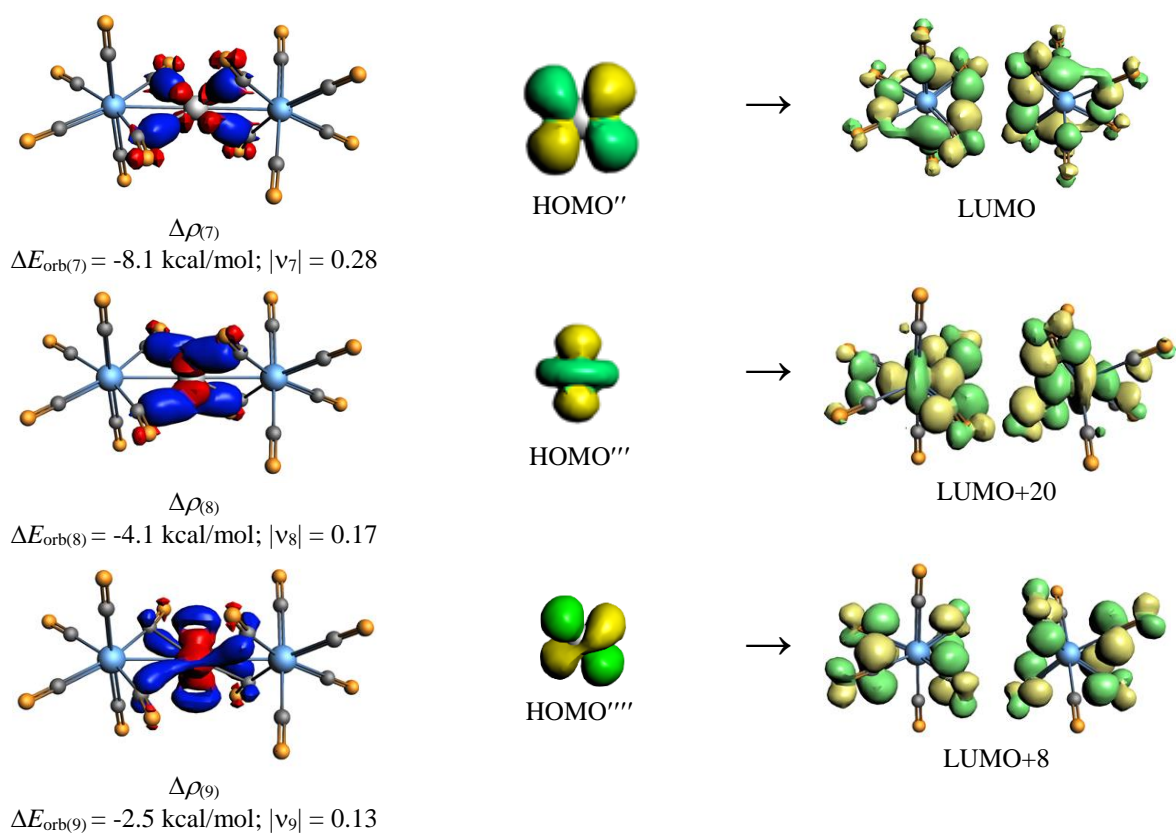




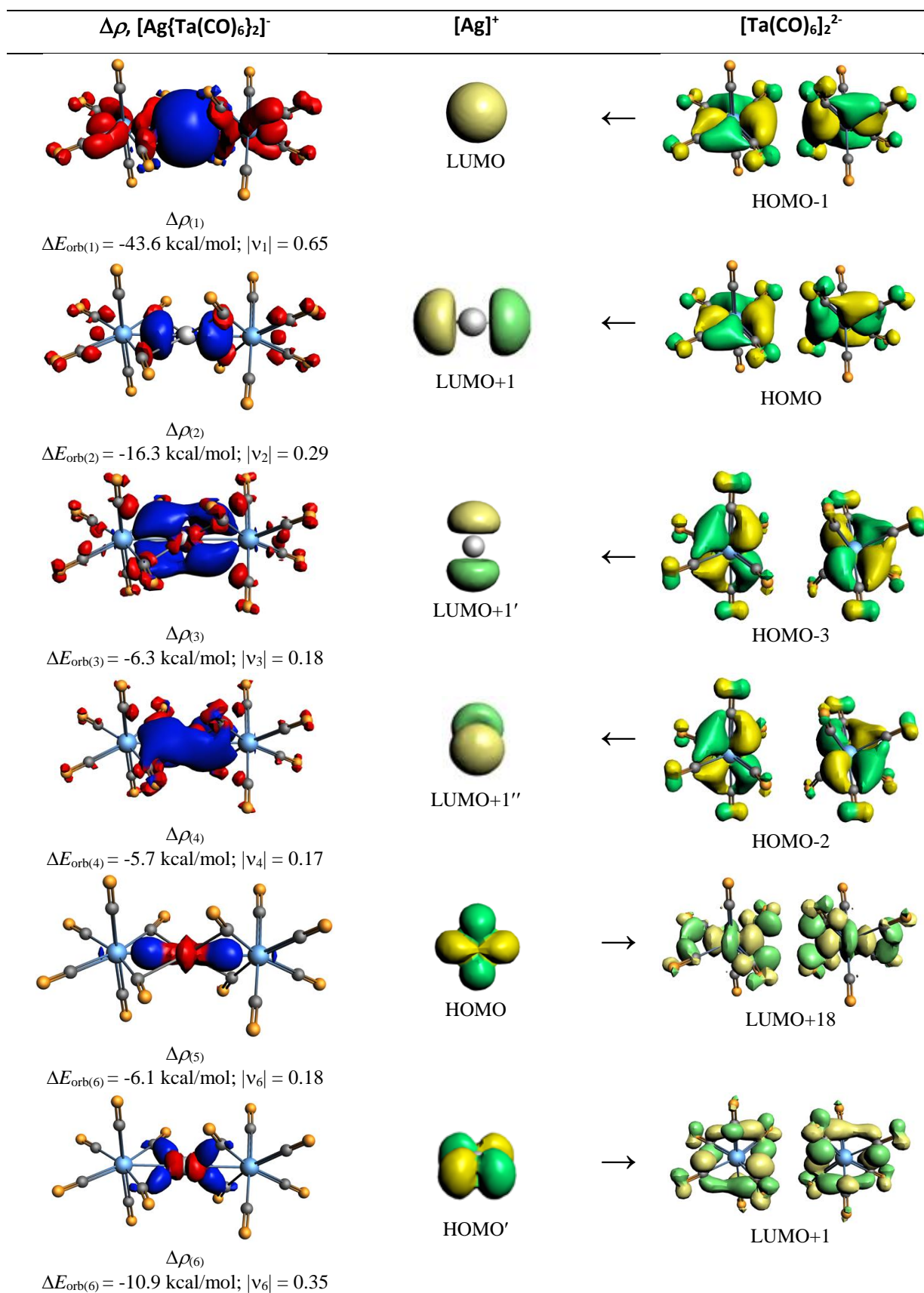
**S-Figure 7.** The shape of the deformation densities  $\Delta\rho_{(1)-(5)}$  that correspond to  $\Delta E_{\text{orb}(1)-(5)}$ , and the fragments orbitals of  $[\text{Ag}]^+$  and  $[\text{V}(\text{CO})_6]^{2-}$  in the singlet state at the BP86-D3(BJ)/TZ2P level. Isosurface values are 0.001 au. The eigenvalues  $|v_n|$  give the size of the charge migration in e. The direction of the charge flow of the deformation densities is red $\rightarrow$ blue.

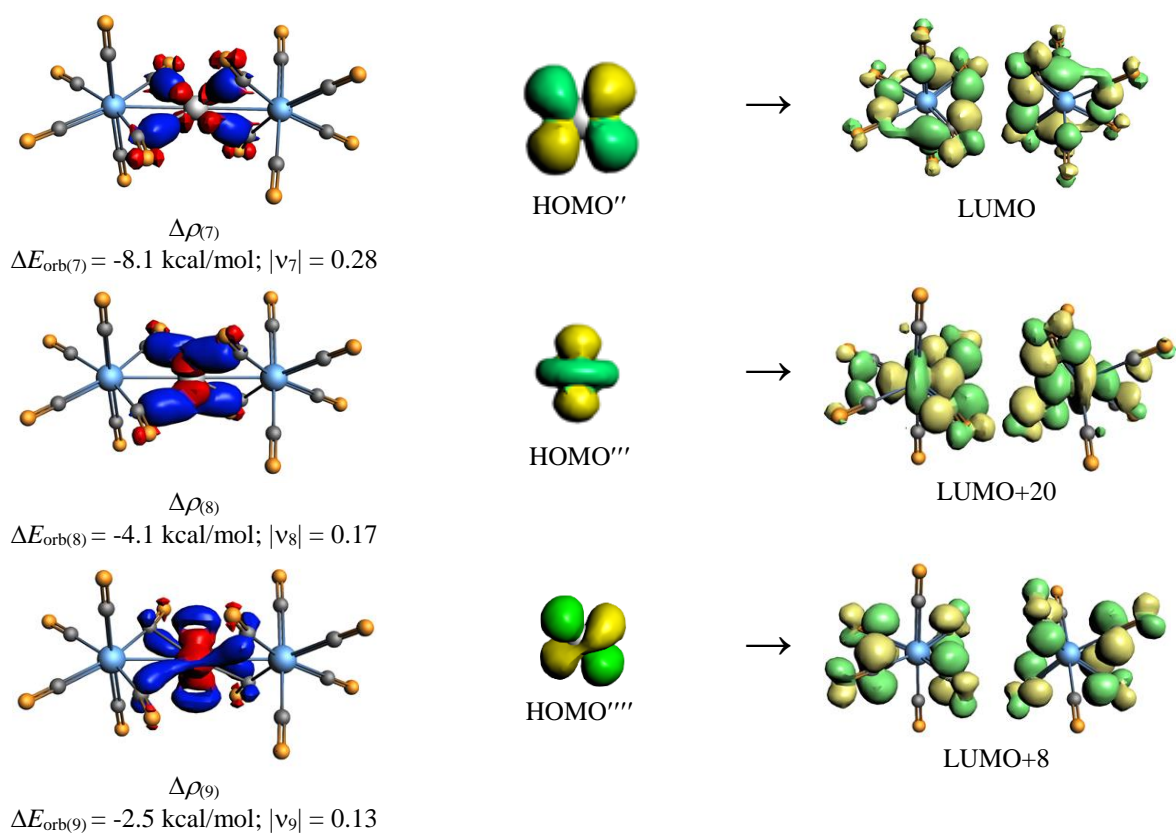






**S-Figure 8.** The shape of the deformation densities  $\Delta\rho_{(1)-(5)}$  that correspond to  $\Delta E_{\text{orb}(1)-(5)}$ , and the fragments orbitals of  $[\text{Ag}]^+$  and  $[\text{Nb}(\text{CO})_6]_2^{2-}$  in the singlet state at the BP86-D3(BJ)/TZ2P level. Isosurface values are 0.001 au. The eigenvalues  $|v_n|$  give the size of the charge migration in e. The direction of the charge flow of the deformation densities is red→blue.





**S-Figure S.** The shape of the deformation densities  $\Delta\rho_{(1)-(5)}$  that correspond to  $\Delta E_{\text{orb}(1)-(5)}$ , and the fragments orbitals of  $[\text{Ag}]^+$  and  $[\text{Ta}(\text{CO})_6]_2^{2-}$  in the singlet state at the BP86-D3(BJ)/TZ2P level. Isosurface values are 0.001 au. The eigenvalues  $|v_n|$  give the size of the charge migration in e. The direction of the charge flow of the deformation densities is red→blue.

## References to the S.I.

- [1] G. Saielli, R. Bini, A. Bagno, *RSC Adv.* **2014**, *4*, 41605.
- [2] V. Wray, L. Ernst, E. Lustig, *J. Magn. Reson.* **1977**, *27*, 1.
- [3] SAINT V8.37A **2015**, Bruker AXS, Madison, Wisconsin, USA.
- [4] L. Krause, R. Herbst-Irmer, G. M. Sheldrick, D. Stalke, *J. Appl. Crystallogr.* **2015**, *48*, 3.
- [5] G. M. Sheldrick, *Acta Cryst. A* **2015**, *71*, 3.
- [6] G. M. Sheldrick, *Acta Cryst. A* **2008**, *64*, 112.
- [7] G. M. Sheldrick, *Acta Cryst. C* **2015**, *71*, 3.
- [8] C. B. Hübschle, G. M. Sheldrick, B. Dittrich, *J. Appl. Crystallogr.* **2011**, *44*, 1281.
- [9] D. Kratzert, J. J. Holstein, I. Krossing, *J. Appl. Crystallogr.* **2015**, *48*, 933.
- [10] C. F. Macrae, I. J. Bruno, J. A. Chisholm, P. R. Edgington, P. McCabe, E. Pidcock, L. Rodriguez-Monge, R. Taylor, J. van de Streek, P. A. Wood, *J. Appl. Crystallogr.* **2008**, *41*, 466.
- [11] O. V. Dolomanov, L. J. Bourhis, R. J. Gildea, J. A. K. Howard, H. Puschmann, *J. Appl. Crystallogr.* **2009**, *42*, 339.
- [12] a) R. Ahlrichs, M. Bär, M. Häser, H. Horn, C. Kölmel, *Chem. Phys. Lett.* **1989**, *162*, 165; b) O. Treutler, R. Ahlrichs, *J. Chem. Phys.* **1995**, *102*, 346.
- [13] a) J. P. Perdew, *Phys. Rev. B* **1986**, *33*, 8822; b) J. P. Perdew, *Phys. Rev. B* **1986**, *34*, 7406.
- [14] a) M. Sierka, A. Hogekamp, R. Ahlrichs, *J. Chem. Phys.* **2003**, *118*, 9136; b) R. Ahlrichs, *Phys. Chem. Chem. Phys.* **2004**, *6*, 5119.
- [15] F. Weigend, R. Ahlrichs, *Phys. Chem. Chem. Phys.* **2005**, *7*, 3297.
- [16] a) S. Grimme, J. Antony, S. Ehrlich, H. Krieg, *J. Chem. Phys.* **2010**, *132*, 154104; b) S. Grimme, S. Ehrlich, L. Goerigk, *J. Comput. Chem.* **2011**, *32*, 1456.
- [17] P. Deglmann, F. Furche, R. Ahlrichs, *Chem. Phys. Lett.* **2002**, *362*, 511.
- [18] A. J. Lehner, N. Trapp, H. Scherer, I. Krossing, *Dalton Trans.* **2011**, *40*, 1448.